OPEN

Emerging Microbes and Infections (2014) 3, e35; doi:10.1038/emi.2014.35

www.nature.com/emi

ORIGINAL ARTICLE

A neonatal gnotobiotic pig model of human enterovirus 71 infection and associated immune responses

Xingdong Yang[1], Guohua Li[1], Ke Wen[1], Tammy Bui[1], Fangning Liu[1], Jacob Kocher[1], Bernard S Jortner[1], Marlice Vonck[1], Kevin Pelzer[1], Jie Deng[2], Runan Zhu[2], Yuyun Li[2], Yuan Qian[2] and Lijuan Yuan[1]

Vaccine development and pathogenesis studies for human enterovirus 71 are limited by a lack of suitable animal models. Here, we report the development of a novel neonatal gnotobiotic pig model using the non-pig-adapted neurovirulent human enterovirus 71 strain BJ110, which has a C4 genotype. Porcine small intestinal epithelial cells, peripheral blood mononuclear cells and neural cells were infected *in vitro*. Oral and combined oral–nasal infection of 5-day-old neonatal gnotobiotic pigs with 5×10^8 fluorescence forming units (FFU) resulted in shedding up to 18 days post-infection, with viral titers in rectal swab samples peaking at 2.22×10^8 viral RNA copies/mL. Viral capsid proteins were detected in enterocytes within the small intestines on post-infection days (PIDs) 7 and 14. Additionally, viral RNA was detected in intestinal and extra-intestinal tissues, including the central nervous system, the lung and cardiac muscle. The infected neonatal gnotobiotic pigs developed fever, forelimb weakness, rapid breathing and some hand, foot and mouth disease symptoms. Flow cytometry analysis revealed increased frequencies of both $CD4^+$ and $CD8^+$ IFN-γ-producing T cells in the brain and the blood on PID 14, but reduced frequencies were observed in the lung. Furthermore, high titers of serum virus-neutralizing antibodies were generated in both orally and combined oral–nasally infected pigs on PIDs 7, 14, 21 and 28. Together, these results demonstrate that neonatal gnotobiotic pigs represent a novel animal model for evaluating vaccines for human enterovirus 71 and for understanding the pathogenesis of this virus and the associated immune responses.
Emerging Microbes and Infections (2014) **3,** e35; doi:10.1038/emi.2014.35; published online 21 May 2014

Keywords: adaptive immune responses; animal model; human enterovirus 71; neonatal gnotobiotic pigs; pathogenesis; vaccine evaluation

INTRODUCTION

Human enterovirus 71 (EV71) is a small, non-enveloped, positive-sense, single-stranded RNA virus. EV71 is a member of the human enterovirus A species and belongs to the *Picornaviridae* family. This virus causes human hand, foot and mouth disease (HFMD), which is frequently associated with severe and sometimes fatal neurological and respiratory disease. Most EV71 infections are asymptomatic or cause only mild and self-limiting HFMD symptoms, such as fever, diarrhea, skin rash, herpangina and vomiting. However, complicated cases with neurological symptoms, such as cerebellar ataxia, poliomyelitis-like syndrome and acute flaccid paralysis, as well as pulmonary edema and hemorrhages, which are associated with most deaths that occur as a result of EV71 infection, have been frequently documented during major outbreaks.[1–3] With the eradication of poliovirus in most parts of the world, EV71 is currently the most important neurovirulent enterovirus. EV71 infections result in more than a million cases of HFMD and hundreds of deaths in infants and young children annually, with the highest incidence and mortality rates observed in children between 6 and 23 months of age.[1,4] However, no anti-viral therapies or vaccines are currently available for EV71. An effective vaccine and effective antiviral drugs are urgently needed to reduce EV71-induced morbidity and mortality. The pathogenesis of EV71 remains unknown, increasing the difficulty of preventative and therapeutic drug development.

Non-human primate and mouse models are commonly used to study EV71 infection. However, both types of animal models have significant limitations. With respect to the primate models, the monkeys used in most studies are older than the age range (i.e., 6 months–3 years) of infants during which most severe and fatal EV71 infections occur, limiting the effectiveness of these animals for modeling the pathogenic events and immune responses associated with severe EV71 infections in human infants. In addition, these primate models were established primarily using alternative inoculation routes rather than oral or nasal inoculation, which are the natural infection routes for EV71.[5–9] Furthermore, the economic and ethical issues associated with primate models greatly limit the utility of such models. Mice represent the most frequently used species for establishing animal models for the study of EV71 infection. While many studies on vaccines, antiviral drugs and pathogenesis have been conducted in mice, no mouse models have replicated the observed respiratory symptoms and lung lesions, such as pulmonary hemorrhage and edema, using any inoculation route.[10,11] In addition, mice older than 2 weeks have not been successfully infected with EV71 to date, despite the use of immune-deficient mice[12] and EV71 receptor transgenic mice.[13] The lack of infection in older mice prevents the study of protective immunity induced by vaccines in these models. Therefore, better animal models are needed for testing vaccines and evaluating therapeutic approaches for EV71 infection and disease.

[1]Department of Biomedical Sciences and Pathobiology, Virginia–Maryland Regional College of Veterinary Medicine, Virginia Polytechnic Institute and State University, Blacksburg, VA 24061-0913, USA and [2]Laboratory of Virology, Capital Institute of Pediatrics, Beijing 100020, China
Correspondence: LJ Yuan
E-mail: lyuan@vt.edu
Received 28 October 2013; revised 10 February 2014; accepted 25 March 2014

Pigs are widely used to study a variety of human diseases because these animals are similar to humans with respect to anatomy, physiology, genetics and immune responses.[14] Of the many immune system parameters that have been evaluated, less than 10% of the murine immune system is similar to the human immune system; in contrast, more than 80% of the porcine immune system is similar to the human immune system.[14] This similarity makes pigs a better model than mice for evaluating human infectious diseases, immune responses and vaccine development. Previous studies performed by our laboratory and other groups used gnotobiotic pigs to study rotavirus and norovirus infections and demonstrated that neonatal gnotobiotic pigs can be successfully used to model human enteric viral infections.[15–19] Furthermore, several receptors for EV71 have been identified; these receptors include P-selectin glycoprotein ligand-1,[20] scavenger receptor class B member 2[21] and sialylated glycans.[22] Conserved proteins that are functionally homologous to these receptors have been described in pigs.[23,24] Thus, we hypothesized that neonatal gnotobiotic pigs may be susceptible to EV71 infection and provide a good animal model.

In this study, we infected a porcine intestinal epithelial cell line (i.e., IPEC-J2), peripheral blood mononuclear cells (PBMCs), neural cells and 5-day-old neonatal gnotobiotic pigs with the recently isolated C4-genotype neurovirulent EV71 strain BJ110 via the oral or combined oral–nasal routes. Clinical signs, virus shedding, virus tissue distribution, histopathology, IFN-γ-producing T-cell responses and serum neutralizing antibody titers were studied to establish the neonatal gnotobiotic pig as a novel animal model for EV71 infection.

MATERIALS AND METHODS

Cell cultures

Vero cells (ATCC, Manassas, VA, USA) were cultured in Dulbecco's modified Eagle medium supplemented with 2% fetal bovine serum, 1% penicillin and 1% streptomycin, according to the vendor's instructions. The IPEC-J2 cell line was a generous gift from Dr Anthony Blikslager (North Carolina State University, Raleigh, NC, USA) and was previously cultured in our laboratory.[25] PBMCs were isolated from neonatal pigs as previously described[26] and were cultured in the same medium as Vero cells. Pig neural cells were isolated from neonatal pig brains using a neural tissue dissociation kit (Miltenyi Biotec, Bergisch Gladbach, Germany) and were cultured in Neurobasal-A medium (Gibco, Grand Island, NY, USA) supplemented with 2% B27 and 1% 0.5 mM glutamine. Cultures of PBMCs and neural cells were confirmed based on morphology via light microscopy.

Virus inoculum preparation

The BJ110 (also called s110) strain of EV71 was isolated from a young male patient who was severely affected by EV71-induced neurological symptoms in Beijing, China in 2008.[12] The third passage of the BJ110 strain in Vero cells was used in the current study. The virus has not undergone any passages in pigs. EV71-infected Vero cells were infected at a multiplicity of infection (MOI) of 0.1 and cultured for 3 days at 37 ℃ with 5% CO_2. After two freeze–thaw cycles at −20 ℃, cell debris was removed by centrifugation at 700*g* and 4 ℃ for 10 min. The supernatant was collected, concentrated and semipurified by ultracentrifugation through a 35% sucrose cushion at 140 000*g* and 4 ℃ for 4 h using an SW28 rotor in a Beckman Coulter Optima-L90K ultracentrifuge (Beckman Coulter, Brea, CA, USA) prior to storage at −80 ℃. Virus titers were determined using a cell culture immunofluorescence (CCIF) assay. Immediately before inoculation, the virus was diluted to an appropriate concentration in Dulbecco's modified Eagle medium containing 1% penicillin and 1% streptomycin.

Cell culture immunofluorescence

Monolayers of Vero cells cultured in 96-well plates were infected with 10-fold serially diluted virus inocula or processed rectal swab samples and incubated at 37 ℃ and 5% CO_2 for 18 h. After washing three times with phosphate-buffered saline (PBS, pH 8.0), the EV71-infected cells were fixed and permeabilized with 80% acetone for 10 min at room temperature and subsequently air-dried. After washing, 50 μL of a mouse anti-EV71 antibody (Abcam, Cambridge, MA, USA) diluted 1 : 1000 with PBS plus 1% bovine serum albumin (BSA) was added into each well. The plates were then incubated for 1 h at 37 ℃. After washing, the plates were incubated with 50 μL of a goat anti-mouse IgG1 antibody labeled with fluorescein isothiocyanate (Sigma-Aldrich, St Louis, MO, USA) for 1 h at 37 ℃. Finally, the plates were mounted with glycerol and examined under a Nikon Eclipse TS100 fluorescence microscope (Nikon, Tokyo, Japan). The number of fluorescent cells in each well was recorded, and the virus titer was reported as fluorescence-forming units (FFU)/mL. The protocol for assessing the infectivity of EV71 in pig primary cell cultures was the same as the protocol described above, except porcine cell cultures were used in place of Vero cell cultures.

Reverse transcription-polymerase chain reaction (RT-PCR) and Taqman real-time PCR

RT-PCR was used to identify the EV71 virus and to detect virus shedding in rectal swab samples. The primer EV71-1 (5′-ATA ATA GCA YTR GCG GCA GCC CA-3′) was previously used in Dr Qian's lab, and the primer EVVP1-R (5′-AGC TGT GCT ATG TGA ATT AGG AA-3′) was described in a previous publication.[27] Reverse transcription was completed at 55 ℃ for 60 min using a Bio-Rad MyCycler thermal cycler (Bio-Rad Laboratories, Inc. Hercules, CA, USA). The PCR cycling conditions were as follows: an initial denaturation at 95 ℃ for 3 min, 35 cycles of 95 ℃ for 20 s, 55 ℃ for 20 s and 68 ℃ for 20 s, and a final elongation at 68 ℃ for 7 min. The 317 bp RT-PCR products were analyzed in 1% gels and subsequently purified and sequenced. The obtained sequences were then compared to the *VP1* sequence of the BJ110 strain in GenBank (Accession NO HM002486.1).

A two-step Taqman real-time PCR was used to quantify the EV71 RNA copies in rectal swab and tissue samples from inoculated neonatal Gnotobiotic pigs. A primer pair (i.e., EV71VP14F: 5′-GGA GAT AGC GTG AGC AGA GC-3′ and EV71VP14R: 5′-ACA GCG TGT CTC AAT CAT GC-3′) and a Taqman probe (i.e., [6-FAM]-TCA CTC ACG CTC TAC CAG CAC CCA-BHQ1) specific for the BJ110 strain of EV71 were designed based on the *VP1* gene sequence of the BJ110 strain of EV71 using the OligoPerfect Designer (Life Technologies, Carlsbad, CA, USA) and were ordered from the same company. The reverse transcription step used the same RT-PCR protocol described above, except different primers were used. Taqman real-time PCR was conducted in a Bio-Rad iQ5 real-time PCR machine (Bio-Rad Laboratories). The 25 μL reaction volume consisted of 12.5 μL of 2× Sensimix buffer (Bioline, Taunton, MA, USA), 1 μL of 10 μM EV71VP14F, 1 μL of 10 μM EV71VP14R, 0.5 μL of 10 μM Taqman Probe, 2.5 μL of cDNA template and 7.5 μL of ddH_2O. The PCR conditions were as follows: 1 cycle of 95 ℃ for 10 min and 40 cycles of 95 ℃ for 10 s and 60 ℃ for 60 s, with real-time detection at the end of each cycle. To quantify EV71 RNA copies, a linear standard curve was also generated during each assay using serial dilutions of an EV71 DNA standard by adjusting the standard to a concentration gradient of 1×10^8 copies/μL to 1×10^0 copies/μL. The detection limitation was 100 copies.

Infection of neonatal gnotobiotic pigs

Near-term pigs of the Large White cross breed were derived by hysterectomy and maintained in germ-free isolator units as described

previously.[28] In the *in vivo* study, specific doses of the EV71 BJ110 strain viral inocula diluted in Diluent #5 (i.e., MEM containing 1% penicillin, 1% streptomycin and 1% HEPES) were administered to 5-day-old gnotobiotic piglets via the oral (O) or combined oral–nasal (O/N) route to test the infectivity of EV71 in neonatal gnotobiotic pigs (Table 1). Control pigs were given an equal amount of Diluent #5. Sterilized IPTT-300 microchips (BioMedic Data Systems, Inc., Seaford, DE, USA) were implanted subcutaneously behind the ear of all pigs to measure body temperature. Clinical signs and body temperature were observed twice daily until euthanasia. Rectal swabs were collected daily to detect virus shedding. Upon euthanasia, organs and tissues were examined for gross lesions and various tissues were collected for histopathology, immunohistochemistry, RNA isolation, and cell isolation for *in vitro* cell culture and flow cytometry analysis. Blood was sampled weekly from the jugular vein of each pig to monitor serum neutralizing antibody titers. Rectal swabs were collected weekly to monitor sterility using blood agar plates and thioglycollate medium. All animal protocols were reviewed and approved by the Institutional Animal Care and Use Committee of Virginia Polytechnic Institute and State University.

Histopathology

The tissues harvested from euthanized pigs were immediately immersion-fixed in 3.7% paraformaldehyde (MP Biomedicals, Santa Ana, CA, USA) for 24 h at room temperature. The fixed tissues were trimmed, paraffin-embedded, sectioned, deparaffinized, rehydrated and stained with hematoxylin and eosin. Additionally, fixed small intestinal tissues were resin-embedded and stained with toluidine blue. The resulting sections were examined under a light microscope.

Immunohistochemistry

Unstained tissue slides from the histopathology study were used for immunohistochemistry. This analysis used the same primary and secondary antibodies as the CCIF assay described above. Briefly, deparaffinized and rehydrated slides were digested with IHC proteinase K (EMD Millipore, Darmstadt, Germany) for 20 min at room temperature. After washing twice in Tris-buffered saline (TBS)–0.1% Triton X-100 for 5 min, the slides were blocked with 10% normal goat serum in TBS–1% BSA for 1 h at room temperature. A primary mouse anti-EV71 monoclonal antibody diluted 1∶1000 in TBS–1% BSA was added, and the slides were incubated overnight at 4 ℃. After washing twice in TBS–Triton X 100 for 5 min, a fluorescein isothiocyanate-conjugated secondary goat anti-mouse IgG diluted 1∶128 in TBS–1% BSA was added; the slides were then incubated for 2 h at room temperature. All incubation steps were conducted in a humidified chamber. After counterstaining in propidium iodide (Invitrogen, Grand Island, NY, USA) for 30 min at room temperature, the slides were mounted with VectaShield mounting medium (Vector Laboratories Inc., Burlingame, CA, USA) and examined under a fluorescent microscope.

Flow cytometry

The frequencies of IFN-γ-producing $CD3^+CD4^+$ and $CD3^+CD8^+$ T cells among the $CD3^+$ lymphocytes in various tissues (i.e., ileum, spleen, blood, lung and brain) were determined using intracellular staining and flow cytometry. Sample collection, sample processing and flow cytometry data collection and analysis were conducted as described in a previous publication.[16] Mononuclear cells from the lung and brain were isolated using the same procedure that was previously described for the spleen.[26] The mononuclear cells were stimulated *in vitro* with 10 μg/mL of semi-purified EV71 antigen or mock-stimulated for 17 h before being subjected to intracellular staining.[16]

Viral neutralization assay

The virus neutralization assay was performed according to a previously described protocol, with some modifications.[29] Briefly, Vero cells were cultured in cell culture medium in 96-well plates for 4 days. Serially diluted heat-inactivated serum samples were mixed 1∶1 with a fixed virus dilution (i.e., 100 FFU/50 μL) and incubated at 37 ℃ for 1 h. Prior to infection, the medium was discarded and each well was washed once with PBS. A 100 μL serum/virus mixture was subsequently added to each well. Duplicate wells were infected for each serum dilution. After incubation at 37 ℃ for 24 h, the plates were fixed with 80% acetone inside a chemical hood at room temperature for exactly 10 min. After washing the plates once with PBS+0.05% Tween 20 (pH 7.4) for 2 min, a 1∶1000 dilution of a mouse anti-EV71 VP1 monoclonal antibody (Abcam, Cambridge, MA, USA) in PBS+1% BSA and a 1∶1000 dilution of the goat polyclonal secondary antibody to mouse IgG-H&L conjugated to horseradish peroxidase (Abcam) in PBS+1% BSA were added sequentially and incubated for 1 h at 37 ℃. After incubation with each antibody, the plates were washed three times with PBS+0.05% Tween 20. Subsequently, 100 μL/well of an aminoethylcarbazole solution (Sigma-Aldrich) was added and incubated at room temperature for 15–30 min, depending on color development. The aminoethylcarbazole solution was then aspirated and 200 μL/well of PBS was added to stop the reaction. The plates were examined under a light microscope. The cytoplasm rather than the nucleus of an infected cell is stained red. The highest dilution at which complete neutralization (i.e., 0 red cells in the well) was achieved was recorded as the serum EV71-neutralizing titer.

Statistical analysis

The Kruskal–Wallis test was performed to compare body temperature, IFN-γ-producing $CD4^+$ and $CD8^+$ T-cell frequencies and virus-neutralizing antibody titers between the EV71-inoculated and control groups using SAS 9.3 software (SAS Institute Inc. Cary, NC, USA). Differences for which $P<0.05$ were considered statistically significant.

RESULTS

Identification of the EV71 BJ110 strain virus inoculum

EV71 was identified using RT-PCR, cytopathic effects (CPEs) and CCIF (Figures 1A a–d). The size of the RT-PCR product was 314 bp, and the sequence of this product matches the *VP1* gene sequence of the EV71 BJ110 strain (GenBank: HM002486.1) (data not shown). CPEs characteristic of EV71, including rounding, aggregation, detaching and

Table 1 Summary of virus shedding in neonatal gnotobiotic pigs infected with the human enterovirus 71 BJ110 strain

Inoculum	Inoculation route	Dosage (FFU)	Euthanasia	Number of pigs infected	Shedding period	Peak titer (RNA copies/mL)	Peak of virus shedding
EV71 BJ110	Oral–nasal	4.5×10^8–5.0×10^7	PID7/14/21	4/4	PID1-12	3.68×10^6	PID1
EV71 BJ110	Oral	5.0×10^8	PID7/14/21	4/4	PID1-18	2.22×10^8	PID6
Diluent	Oral	N/A	PID7/14/21	0/4	N/A	NA	NA

PID, post-infection day.

apoptosis, were observed in Vero cells; these effects typically began to appear 24 h after infection at an MOI of 1. EV71 viruses were further detected using an anti-EV71 capsid protein VP1-specific monoclonal antibody in CCIF (Figure 1A d). Based on these results, we confirmed that the virus stock was the EV71 BJ110 strain.

EV71 infects porcine cell cultures *in vitro*

The infectivity of EV71 was tested using porcine intestinal epithelial cells (i.e., IPEC-J2 cells), PBMCs and neural cells. The human EV71 BJ110 strain infected all three porcine cell cultures (Figure 1B). Consistent with most positive-strand RNA viruses, virus replication and assembly were detected in the cytoplasm, as indicated by exclusive cytoplasmic fluorescence. Although all three porcine cell cultures were susceptible to EV71 BJ110 strain infection, differences in the efficiency of intracellular viral replication and assembly were observed among these cell types, with the strongest immunofluorescence detected in IPEC-J2 cells, intermediate immunofluorescence detected in PBMCs and the weakest immunofluorescence detected in neural cells. However, no significant CPEs were observed in any of these porcine cell cultures.

To assess the efficiency of EV71 replication in IPEC-J2 cells, viral growth curves in both IPEC-J2 and positive control Vero cells were generated using Taqman real-time PCR. The viral RNA titers in the cell culture medium at different time points after infection at MOIs of 0.1, 1 and 10 are presented in Figure 1C. The extracellular viral titer for Vero cells peaked at 60 h post-infection at MOIs of 1 and 10. However, Vero cells infected at an MOI of 1 reached the highest viral titer, with approximately 1×10^8 RNA copies/mL. Extracellular virus titers for the IPEC-J2 cells peaked at 48 h post-infection at MOIs of 1 and 10. After infection at an MOI of 0.1, the virus titer peak was delayed to 72 h. Similar to the result observed for Vero cells, the highest extracellular viral titer of 1.1×10^5 RNA copies/mL was observed for IPEC-J2 cells infected at an MOI of 1.

Virus shedding and tissue distribution in infected neonatal gnotobiotic pigs

Viral shedding was detected by RT-PCR or Taqman real-time PCR. For both the oral and combined oral–nasal infection groups, virus shedding was detected (Figures 2A and 2B and Table 1). When detected by RT-PCR, virus shedding was detectable from post-infection day (PID) 5 for the orally infected pigs and from PID 1 for the combined oral–nasally infected pigs. Consistent with the RT-PCR results, viral titers peaked between PID 5 and PID 8 for the orally infected pigs, as determined using Taqman real-time PCR. For the combined oral–nasally infected pigs, virus titer peaks ranged from PID 1 and PID 4 and were typically lower than the peaks observed in the orally infected pigs. Both groups began shedding virus from PID 1 and continued until PID 18 and PID 12 (ranging from 2.16×10^3 to 2.22×10^8 RNA copies/mL) for the orally and the combined oral–nasally infected pigs, respectively. No viral RNA was detected in the control group. The EV71 VP1 protein was detected at concentrations up to 5 ng/mL in rectal swab samples from both orally and combined

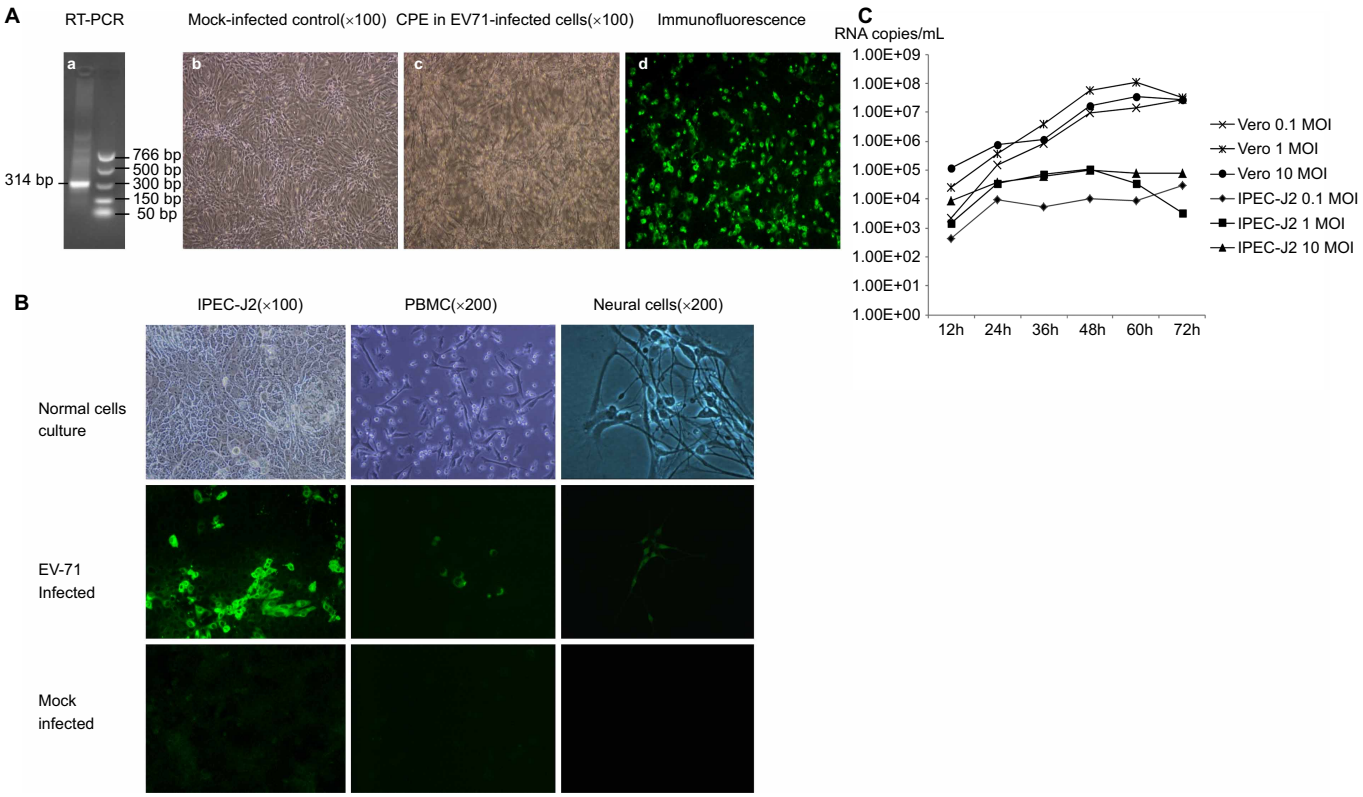

Figure 1 The human EV71 BJ110 strain infects and replicates in pig intestinal epithelial cells, PBMCs and neural cell culture *in vitro*. (**A**) Identification of virus inoculum. (**a**) RT-PCR detection of the EV71 BJ110 strain. The positive PCR products were purified and sequenced. The sequence shares 100% identity with the published EV71 BJ110 strain *VP1* gene sequence. (**b**) Mock-infected Vero cell culture. (**c**) CPE in Vero cells 72 h post-inoculation with the EV71 BJ110 strain at a MOI of 10. (**d**) EV71-infected Vero cells were detected using CCIF. (**B**) Porcine cell cultures can be infected by the EV71 BJ110 strain. EV71 was detected in IPEC-J2 cells, PBMCs and neural cells using CCIF. (**C**) Growth curves for the EV71 BJ110 strain in Vero and IPEC-J2 cells suggest that EV71 infects and replicates efficiently in IPEC-J2 cells.

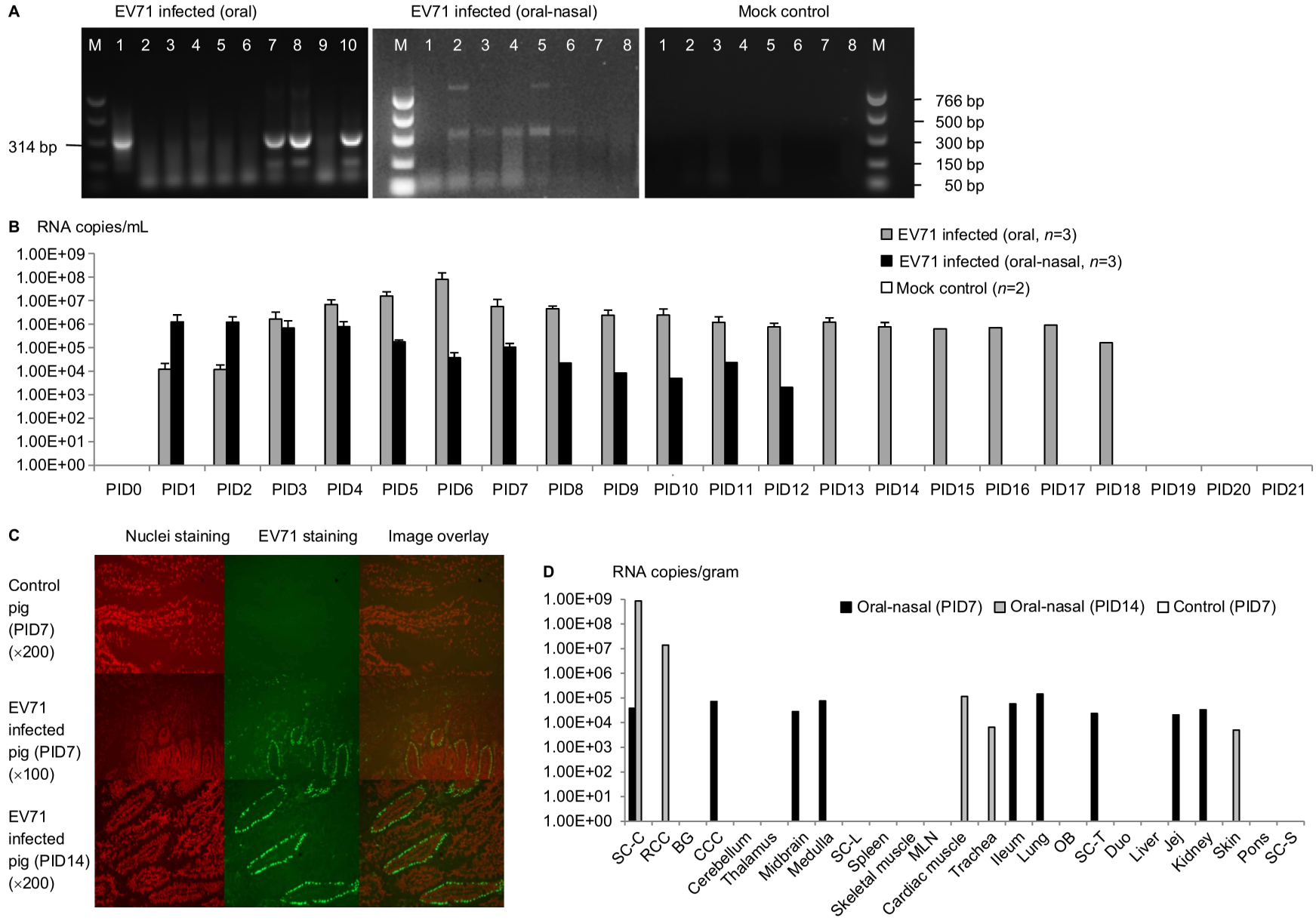

Figure 2 EV71 BJ110 strain fecal shedding, tissue distribution and dynamics in infected neonatal gnotobiotic pigs. (**A**) RT-PCR detection of EV71 in rectal swab samples. Left, RT-PCR detection of EV71 viral RNA in one orally infected pig (M, marker; lane 1, positive control; lanes 2–10, PID 0–8). Middle, RT-PCR detection of EV71 viral RNA in one oral–nasally infected pig (M, marker; lanes 1–8, PID 0–7). Right, RT-PCR detection of EV71 viral RNA in a mock control pig (lanes 1–8, PID 0–7; M, marker). (**B**) Taqman real-time PCR detection of virus shedding in rectal swab samples from different treatment groups. The mean viral RNA titer for each group at a specific time point is presented. The error bar indicates the standard error of the mean. No virus shedding was detected for any mock control group pigs at any time point; therefore, no bars are visible. (**C**) Detection of viral

antigen on PID 7 and PID 14 in the ileum of gnotobiotic pigs infected with the EV71 BJ110 strain through the oral–nasal route at a dose of 5×10^8 FFU by immunofluorescence staining. A mouse anti-EV71 capsid protein VP1 monoclonal antibody (Abcam) was used as the primary antibody, and a goat anti-mouse IgG1 antibody labeled with fluorescein isothiocyanate (Sigma-Aldrich) was used as the secondary antibody. Nuclei were stained red by propidium iodide (Invitrogen). (**D**) Taqman real-time PCR detection of EV71 viral RNA in tissues of infected gnotobiotic pigs at PID 7 or PID 14. The route of inoculation and the euthanasia time (in parentheses) of the pigs are marked in the legends. Viral titers are presented as the mean of two replicates for the same sample. The negative samples are shown as blank on the bar graph. All data are representative of at least two independent experiments. BG, basal ganglia; CCC, caudal cerebral cortex; Duo, duodenum; Jej, jejunum; MLN, mesenteric lymph nodes; OB, olfactory bulb; RCC, rostral cerebral cortex; SC-C, spinal cord-cervical; SC-L, spinal cord-lumbar; SC-T, spinal cord-thoracic; SC-S, spinal cord-sacral.

oral–nasally infected pigs using the EV71 VP1 ELISA kit (Abnova, Taipei City, Taiwan) (data not shown). To detect live and infectious viruses, the CCIF assay was performed; low viral titers (40–160 FFU/mL) were detected in orally infected pigs (data not shown). Therefore, while high viral RNA titers were detected in rectal swab samples, viral proteins or infectious virus particles were not abundantly shed in the EV71-infected pigs.

Virus tissue distribution and titers at different time points after infection were determined using Taqman real-time PCR and immunohistochemistry. For the combined oral–nasally infected pigs, viral capsid proteins were detected in the cytoplasm of enterocytes in the small intestine on PID 7 and PID 14 (Figure 2C). Additionally, a high virus titer was detected in many tissues, including small intestine, central nervous system and lung, in the infected pigs on both PID 7 and 14; in contrast, no viral RNA was detected in the control pigs (Figure 2D). Antigen presence and tissue viral titers were not determined for the orally infected pigs due to a lack of tissue samples.

Clinical signs in pigs mimic human patients

After infection of neonatal gnotobiotic pigs with the EV71 BJ110 strain, clinical signs were monitored twice daily from PID 0 until the time of euthanasia, which ranged from PID 7 to PID 28. Body temperatures in the combined oral–nasally infected group were significantly higher than in the mock control group or in the orally infected group on PID 4, 5 and 6 (Figure 3A). No significant differences in body temperature were observed between the orally infected group and the mock control group at any time points (Figure 3A). As observed in human patients, fever (i.e., body temperature $\geqslant$40 ℃) and lethargy were two of the most frequently observed clinical manifestations among the combined oral–nasally infected pigs (Figure 3A

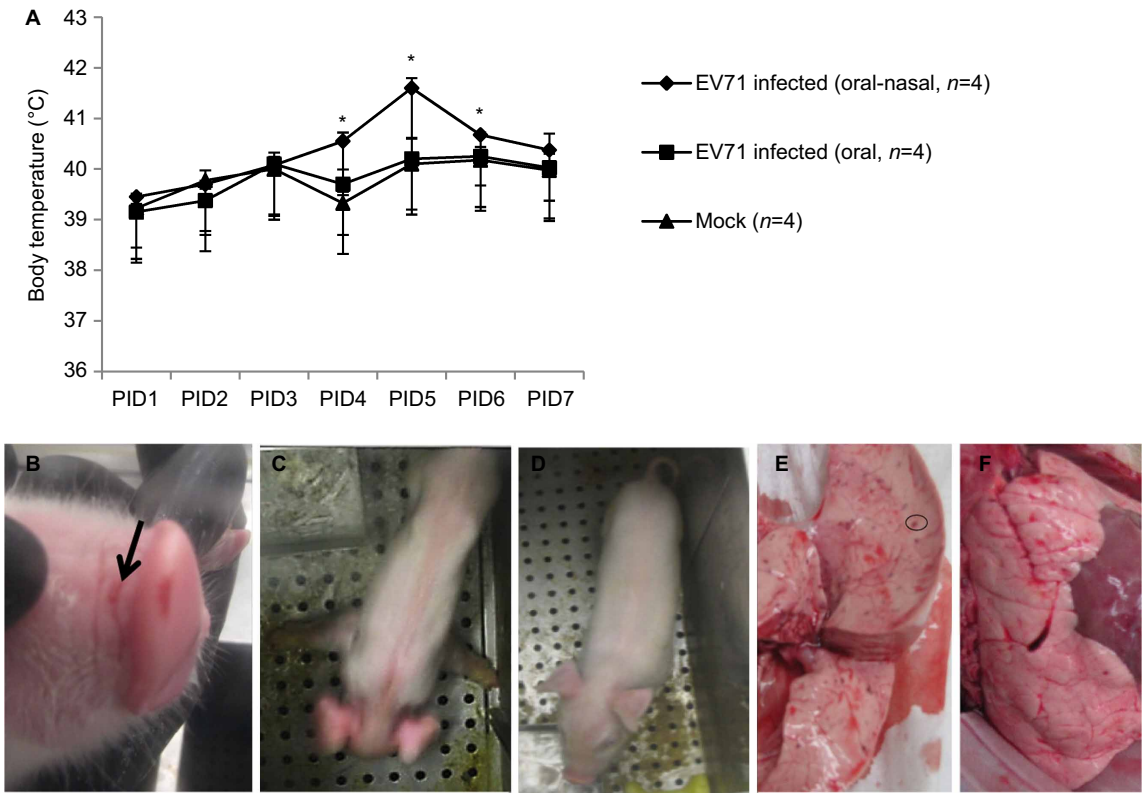

Figure 3 Fever, limb paralysis, vesicles and lung lesions in EV71-infected neonatal gnotobiotic pigs. (**A**) Body temperature in the EV71-infected neonatal gnotobiotic pigs. Body temperature was measured using subcutaneously implanted microchips posterior to the ear. The body temperature at each time point represents an average of three measurements. The normal core body temperature of pigs ranges from 38 to 40 ℃, with an average of 38.8 ℃. A temperature higher than 40 ℃ is considered a fever. (**B**) Vesicles (indicated by black arrow) on the snouts of EV71-infected neonatal gnotobiotic pigs. (**C**) Forelimb weakness in neonatal gnotobiotic pigs infected with the EV71 BJ110 strain. (**D**) An age-matched mock-infected control neonatal gnotobiotic pig. B (**E**) Multifocal mottling with petechial hemorrhages (indicated by the circle) in the lung was observed in an oral-nasally inoculated gnotobiotic pig on PID 21. (**F**) Normal lung from a mock-infected gnotobiotic pig. *$P<0.05$, as indicated by the Kruskal–Wallis test.

Table 2 Clinical signs in neonatal gnotobiotic pigs infected with the human enterovirus 71 BJ110 strain

Group	PPD[a]	Inoculation route	Dosage	Virus sheddin[b]	Fever (⩾40 ℃)	Diarrhea	Skin lesion[c]	Respiratory signs[c]	Neurological signs[c]	Frothy mouth
EV71 BJ110	5	Oral-nasal	4.5×10^8 FFU/oral; 5×10^7 FFU/nasal	4/4	4/4	0/4	0/4	4/4	4/4	0/4
EV71 BJ110	5	Oral	5×10^8 FFU/dose	4/4	0/4	0/4	1/4	2/4	2/4	1/4
Control	5	Oral	5 mL Diluent #5[d]	0/4	0/4	0/4	0/4	1/4	0/4	0/4

[a] Postpartum day.
[b] Virus shedding was detected in rectal swabs using real-time PCR.
[c] See a more detailed description of these symptoms in the text.
[d] Diluent #5 is the medium used to dilute the EV71 virus inoculum.

and Table 2). Occasionally, vesicles were present in the snouts of the infected pigs (Figure 3B). The observed neurological signs included limb weakness, particularly forelimb weakness, diminished reflexes, ataxia, myoclonic jerk, convulsions and in some pigs, irritability and involuntary movements of the mouth, facial muscles and ears (Figure 3C). No neurological signs were present in the control pigs (Figure 3D). Respiratory signs, including fast and deep breathing (i.e., tachypnea and hyperpnea), open mouth breathing and peculiar laying position, were observed in six of eight pigs (75%) infected with the EV71 BJ110 strain. These clinical signs were more frequently observed in the combined oral–nasally infected pigs than in the orally infected pigs. However, none of the infected pigs that exhibited neurological and respiratory signs progressed to cardiopulmonary failure or death during the study period. No clinical signs were observed in the mock-infected pigs. In addition, the sterility of the gnotobiotic pigs was monitored weekly by plating rectal swab samples on blood agar plates and thioglycollate medium. All bacterial cultures were negative for all of the gnotobiotic pigs used in this study. This result excludes the possibility that the observed clinical signs were caused by extraneous microbial intestinal infections.

Pathology in neonatal gnotobiotic pigs infected with EV71

Multifocal mottling with petechial hemorrhages and swelling were observed in the lungs (Figures 3E and 3F) in two of eight infected pigs: one orally inoculated pig on PID 29 and one oral–nasally inoculated pig on PID 21. No gross lesions were observed in any other tissues, except for hemorrhages and atrophy of mesenteric lymph nodes.

Histopathological changes were only observed in the lungs, small intestine, particularly in the ileum, and mesenteric lymph nodes of neonatal gnotobiotic pigs infected with EV71 (Figure 4). Peribronchial and alveolar hemorrhage and edema were present, with infiltration of lymphocytes, prominent peribronchiolar lymphoid tissue and thickening of the alveolar septae. Occasional neutrophils were observed in the bronchi. In addition, hemosiderin-laden macrophages were

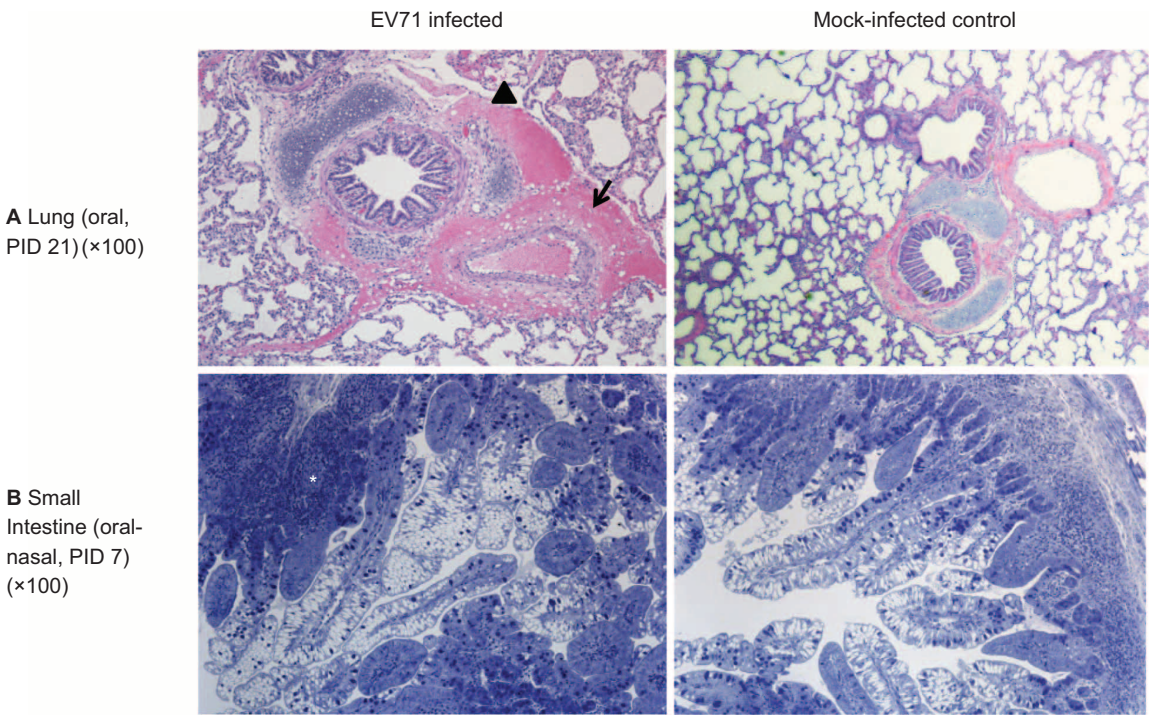

Figure 4 Microscopic lesions in neonatal gnotobiotic pigs infected with the EV71 BJ110 strain. (**A**) The upper panel shows a section of the lung of an orally infected gnotobiotic pig and a mock-infected control on PID 21. The infected pig has peribronchial and perivascular hemorrhage (indicated by the arrow). An adjacent alveolus contains scattered erythrocytes and macrophages (indicated by the black triangle). (**B**) The lower panel shows the small intestine of an oral-nasally infected gnotobiotic pig on PID 7, with a prominent presence of immune cells in the lamina propria and a significantly increased number of Peyer's patches (indicated by the asterisk). Lung tissues were stained with H&E; small intestinal tissues were sections of resin-embedded tissue stained with toluidine blue. H&E, hematoxylin and eosin.

observed in the alveolar space. Hemorrhage and infiltration of lymphocytes were also observed in the pleura. In the small intestine, the EV71-infected pigs exhibited an increased size and number of Peyer's patches and a significantly larger amount of immune cells in the lamina propria. Scattered eosinophils were observed in the mucosa of the duodenum, jejunum and ileum, and vacuolated lymphocytes were noted in the Peyer's patches of the ileum. No severe lesions were present in the intestinal epithelium at the investigated time points (i.e., 7, 14, 21 and 28 days after infection) (Supplementary Figure S1). Prominent hemorrhage, numerous hemosiderin-laden macrophages in the walls of sinuses, a reduction of lymphoid tissue and infiltration of eosinophils were observed in the mesenteric lymph nodes (data not shown). No lesions were observed in any part of the central nervous system, including the cerebral cortex, cerebellum, brainstem and spinal cord. In addition, no microscopic lesions were observed in the other examined tissues, including the heart, skeletal muscle, kidney, spleen, liver and tongue.

Robust adaptive immune responses in EV71-infected pigs

To examine the adaptive immune responses that occur during EV71 infection in neonatal gnotobiotic pigs, the frequencies of virus-specific IFN-γ-producing $CD3^+CD4^+$ and $CD3^+CD8^+$ T cells among the $CD3^+$ lymphocytes in both systemic and local tissues and serum virus-neutralizing antibody titers were analyzed using flow cytometry and a microplate virus neutralization assay, respectively. Representative dot plots of the $CD3^+CD4^+IFN\text{-}\gamma^+$ and $CD3^+CD8^+IFN\text{-}\gamma^+$ T lymphocytes among the total $CD3^+$ mononuclear cells are presented for the blood (Figure 5A). Compared to the mock control group, the combined oral–nasal infection group exhibited higher frequencies of the $CD4^+$ T-cell subset in the blood and the brain. However, lower frequencies of this subset were observed in the lung on both PID 7 and PID 14. For the $CD8^+$ T-cell subset, a higher frequency was induced in the ileum on PID 7 and in the blood and the brain on PID 14. In contrast, the frequency of this subset was reduced in both the brain and the lung on PID 7 and in the lung on PID 14 (Figure 5B). However, the observed changes in the frequencies of both T-cell subsets were not statistically significant.

The results from the serum virus-neutralizing antibody assay demonstrated that significantly higher neutralizing antibody titers were induced in orally inoculated pigs on PID 7, PID 14 and PID 21 compared to the baseline on PID 0 (Figure 5C). Significantly higher antibody titers were also induced in the combined oral–nasally infected pigs on PID 7 and PID 14 compared to the baseline on PID 0. However, significantly higher serum antibody titers were induced in the orally infected pigs than in the combined oral–nasally infected pigs on both PID 7 and PID 14. Serum neutralizing antibody responses were not determined beyond PID 21, except in one orally infected pig that had a slightly reduced titer on PID 28 compared to PID 21.

DISCUSSION

Due to the ongoing extensive and severe EV71 epidemic in Asia, which is associated with high morbidity and mortality rates and a lack of appropriate treatments, effective vaccines and therapeutic drugs must be developed. Substantial progress has been made in our understanding of basic EV71 virology; this progress may facilitate intensive efforts among researchers, governments, and industries to develop vaccines and antiviral drugs that target EV71. For example, the crystal structure of EV71 was recently determined.[30,31] However, one major obstacle that remains is the lack of a reliable working animal model for EV71 infection. In this study, we provide clear evidence that neonatal gnotobiotic pigs can be infected both orally and oral–nasally, resulting in virus shedding patterns, neurological and respiratory signs, and T-cell and antibody responses that mimic human disease. A comparison of the oral infection group to the combined oral–nasal infection group revealed that the oral infection group exhibited higher fecal virus shedding, lower body temperature (i.e., the absence of fever versus fever in the combined oral–nasal infection group), higher serum neutralizing antibodies and less severe clinical signs than the combined oral–nasal infection group. Therefore, gnotobiotic pigs can be used as an alternative animal model for the currently available murine and non-human primate models.

Intestinal epithelial cells, PBMCs and neural cells are important targets for virus infection, replication, dissemination and pathogenesis during EV71 infection. The finding that porcine intestinal IPEC-J2 cells can be infected by the EV71 BJ110 strain suggests that neonatal pigs can be infected orally, as EV71 is known to resist gastric acid in the stomach.[32] Based on the intensity of the immunofluorescent signal, the short time of infection prior to detection (20 h), and the high viral RNA titers in the infected IPEC-J2 cell culture supernatants, EV71 infection appears to be fairly efficient in IPEC-J2 cells. The growth curve of the EV71 BJ110 strain in IPEC-J2 cells further demonstrates that EV71 replicates effectively in porcine intestinal epithelial cells (Figure 1C). Immune cells play an essential role in host defense against EV71 infection, but these cells are also the means by which EV71 spreads and causes lesions and disease in human patients.[32,33] Lymphopenia is associated with EV71-induced pulmonary edema.[34] In our study, porcine PBMCs were also infected by EV71. In a single experiment, porcine neural cells were infected with EV71; however, viral replication in these neural cells was not robust. The infection of porcine neural cell cultures by the EV71 BJ110 strain is consistent with the detection of EV71 viruses in the brains of human patients and the infection of human neuronal cell lines by EV71 *in vitro*.[35,36] However, the pro-inflammatory cytokine responses induced by EV71 may contribute to neurological and pulmonary disease without viral invasion of neurons.[37] Consistent with this idea, we observed increased frequencies of $CD3^+CD4^+IFN\text{-}\gamma^+$ T lymphocytes in the brain on both PID7 and 14 (Figure 5B). Taken together, this finding and the low replication level of EV71 in neural cells may explain the lack of lesions in the central nervous system of the infected neonatal gnotobiotic pigs in the current study. However, because the neural cells used in the current study are different from neurons and because high viral RNA levels were detected in the central nervous system (Figure 2D), we cannot rule out the possibility that EV71 productively infects neurons and the associated neuronal injuries are undetected. Taken together, the *in vitro* infection of pig cell cultures (i.e., IPEC-J2 cells, PBMCs and neural cells) by EV71 supported our *in vivo* results, which demonstrated that neonatal gnotobiotic pigs can be infected with EV71.

To better represent EV71 infection of children less than 3 years old,[38] 5-day-old neonatal gnotobiotic pigs were used in our study. Long-lasting high levels of virus shedding were detected in fecal samples from both orally and combined oral–nasally infected pigs using Taqman real-time PCR. This finding is consistent with our results that demonstrated that more efficient EV71 infection occurs in IPEC-J2 cell culture than in PBMCs; this result suggests that intestinal epithelial cells are the major site of viral replication during EV71 infection in neonatal gnotobiotic pigs. Consistent with the detection of high EV71 shedding titers in fecal samples from the combined oral–nasally inoculated EV71-infected pigs, viral capsid proteins were also detected in the enterocytes of the ileum on PID 7 and PID 14. This result further confirms that EV71 infection and replication in intestinal epithelial

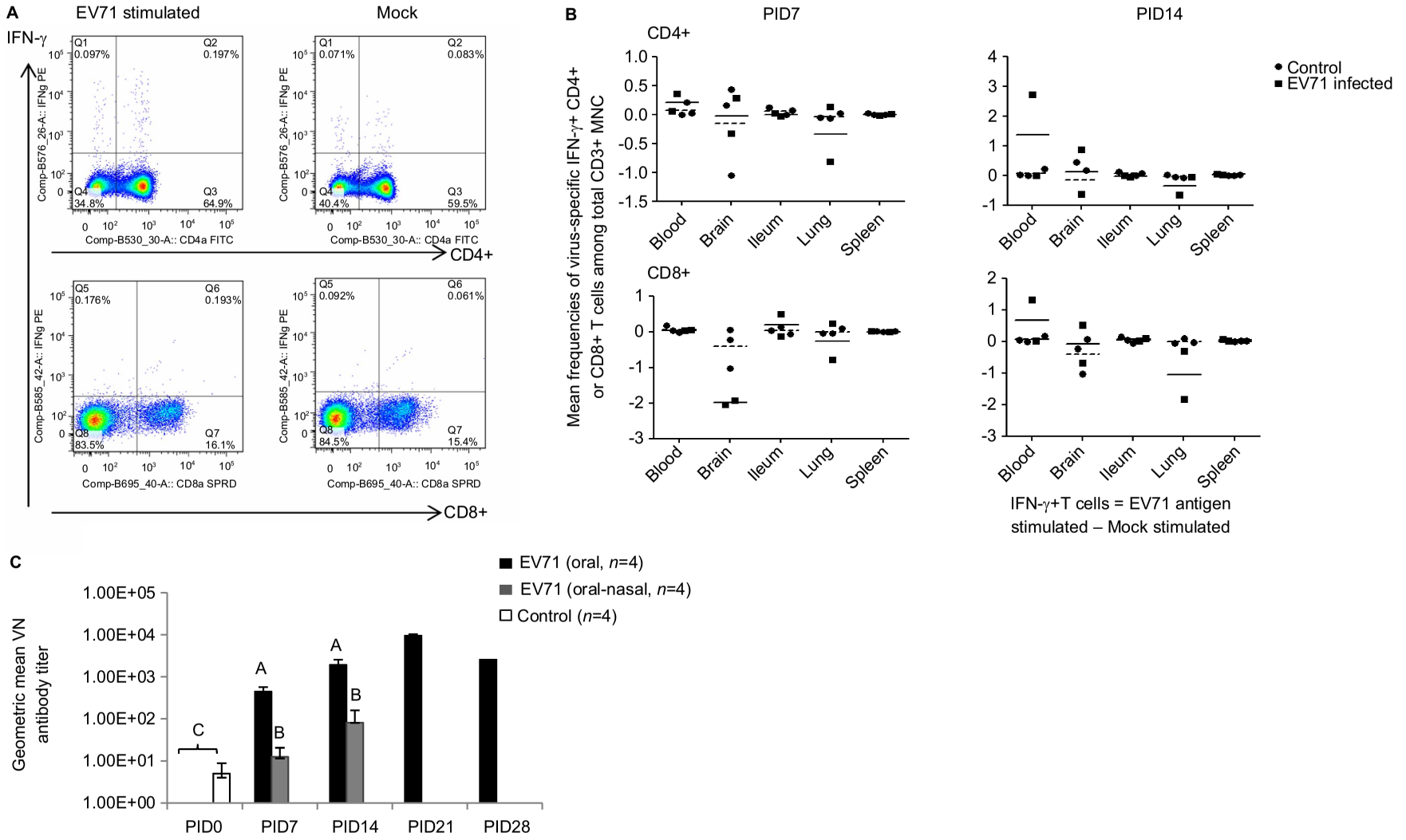

Figure 5 Immune responses during EV71 infection in neonatal gnotobiotic pigs. (**A**) Representative dot plots showing the frequency of $CD3^+CD4^+IFN\text{-}\gamma^+$ and $CD3^+CD8^+IFN\text{-}\gamma^+$ T lymphocytes among the total $CD3^+$ mononuclear cells in the blood. MNCs were stimulated with semi-purified whole EV71 antigen or control medium for 17 h prior to staining. (**B**) The frequency of IFN-γ-producing $CD3^+CD4^+$ and $CD3^+CD8^+$ T cells among the $CD3^+$ mononuclear cells in the ileum, spleen, blood, brain and lung on PID 7 and PID 14 after EV71 BJ110 infection via the oral–nasal route in neonatal gnotobiotic pigs. The mean frequencies were calculated by subtracting the mean frequency value of medium/mock stimulated cells from the mean frequency value of virus-stimulated cells. A positive mean frequency value indicates that IFN-γ production was upregulated upon virus stimulation, whereas a negative mean frequency value indicates that IFN-γ production was downregulated upon virus stimulation. The mean value for the EV71-infected group is indicated by the solid line, and the mean value for the mock control group is indicated by the dashed line. (**C**) Serum neutralizing antibody response in EV71-infected neonatal gnotobiotic pigs. Different uppercase letters (i.e., A, B and C) indicate significant differences between different treatment groups and different time points within the same treatment group. Shared uppercase letters or no letters indicate that no significant differences were observed. (Kruskal–Wallis test, $P<0.05$; $n=4$). MNC, mononuclear cell.

cells is efficient and persistent. In short, these results indicate that oral or combined oral–nasal inoculation of neonatal gnotobiotic pigs with EV71 BJ110 allows EV71 to infect and replicate in intestinal epithelial cells effectively and persistently. This result is significant because the EV71 BJ110 strain has not been passaged in pigs. It remains unknown whether EV71 infects and circulates in pigs under natural environmental conditions. Epidemiological studies of swine populations are needed to examine the zoonotic potential of human EV71.

Similar to human patients, the clinical signs observed in the neonatal gnotobiotic pigs inoculated with EV71 included typical HFMD symptoms, as well as neurological and respiratory symptoms. However, only occasional skin lesions were observed, suggesting that the EV71 BJ110 strain is not intensely dermotropic in pigs. Interestingly, combined oral–nasal infection caused more severe and frequent neurological and respiratory signs than oral infection alone in neonatal gnotobiotic pigs (Table 2). This difference may be caused by the stronger systemic inflammation that is induced by simultaneous stimulation of the mucosal immune system at multiple sites in the combined oral–nasal infection group. This theory is corroborated by the high fever, reduced virus replication and shedding, and resulting lower T cell and serum neutralizing antibody responses observed in this group.

The febrile response that is induced during virus infection is a major defense mechanism for ridding the host of virus replication. Oral inoculation of pigs with EV71 did not induce significant body temperature increases compared to mock-inoculated pigs; this lack of fever may have resulted in the higher titers and longer periods of fecal virus shedding that were observed in these animals. Consequently, the higher viral antigen load induced higher neutralizing antibody titers in the orally inoculated pigs. However, it remains unknown why oral infection by EV71 failed to induce a febrile response in the pigs. The small number of pigs in this group may have been a contributing factor. Additional experiments with a larger number of pigs in each group are needed to address this issue.

While no detailed mechanistic data are available, the following route for the systemic spread of EV71 viruses is likely to occur in the current pig model. Upon oral or combined oral–nasal inoculation, EV71 viruses infect and replicate in small intestinal epithelial cells. Then, EV71 viruses reach the blood circulation, causing viremia and fever. EV71 viruses then spread to target organs, such as the lung, central nervous system, kidney, cardiac muscle and skin, through the blood or lymph circulation systems. After reaching the target organ, EV71 viruses infect and replicate in the cells of the target organ, inducing inflammation or immune responses. These responses are responsible for the removal of the invading viruses. Systemic spread of the virus to different organs occurs at different time points. In particular, the spread of EV71 viruses to the central nervous system results in virus replication in the midbrain, medulla, cervical spinal cord, and caudal cerebral cortex at 7 days post-infection. Replication shifts to the cervical spinal cord and rostral cerebral cortex at 14 days post-infection. Based on the tissue viral RNA titers (Figure 2D) obtained in the current study, it remains unknown how long EV71 viruses persist in different target organs. It is also unclear whether any additional target organs are involved. Future experiments comparing the viral tissue distribution at different time points are necessary to identify differences in the systemic spread of EV71 viruses between the oral and combined oral–nasal infection groups.

Despite the observed clinical signs and the presence of high titers of viral RNA, it remains unclear why no extensive tissue damage or massive inflammation was observed in the central nervous system or in other tissues, including intestinal tissues. This lack of damage may be due to the lack of normal microbiota in these gnotobiotic pigs. The gut microbiota is increasingly recognized as a major contributor to mucosal and systemic inflammation and to diseases.[39] In the lung, the lesions, such as edema and focal hemorrhage, which were observed in two of eight inoculated pigs, have also been observed in fatal EV71 infections in humans.[40] However, these lesions were observed in only 25% of all inoculated pigs and were absent in some pigs that displayed respiratory symptoms. Due to the small number of pigs included in the current study, the possibility that these lung lesions were caused by factors other than EV71 infection alone cannot be ignored. The presence of pulmonary hemorrhage and edema in combination with respiratory and neurological symptoms in one orally infected pig is particularly interesting, as these features are frequently associated with a high mortality rate in young children.[3] These features have only been observed in intracerebrally inoculated monkeys to date.[41] Together, these pathological results indicate that oral or combined oral–nasal infection by neurovirulent EV71 BJ110 in neonatal gnotobiotic pigs can cause respiratory and neurological lesions and clinical signs similar to those observed in human patients.

In addition to virus replication, shedding, clinical signs and pathology, adaptive immune responses are essential parameters in the evaluation of vaccines, the characterization of immunity, the determination of correlates of protective immunity and the study of immunopathogenesis during EV71 infection. To establish the neonatal gnotobiotic pig model, EV71-specific IFN-γ^+ T-cell responses and serum EV71-neutralizing antibody titers were assessed at different time points during EV71 infection. IFN-γ plays a major role in host defense against viral infections. Increased EV71 neurovirulence has also been observed in IFN-γ receptor-deficient mice.[12] Another study used PBMCs from EV71 patients to demonstrate that significantly lower levels of IFN-γ were secreted by PBMCs from patients with pulmonary edema than by PBMCs from patients without pulmonary edema after *in vitro* stimulation with EV71.[42] Consistent with these results, all of the infected pigs in this study, including three pigs that exhibited both respiratory signs and lung lesions, exhibited reduced frequencies of both $CD3^+CD4^+IFN\text{-}\gamma^+$ and $CD3^+CD8^+IFN\text{-}\gamma^+$ T cells in the lung on PID 7 and PID 14. This reduction may have contributed to the neurological and respiratory signs observed in this study. However, as an inflammatory cytokine, IFN-γ can also cause tissue injury and exacerbate EV71 infection. The increased frequencies of both $CD3^+CD4^+IFN\text{-}\gamma^+$ and $CD3^+CD8^+IFN\text{-}\gamma^+$ T cells in the brain are also consistent with a study that reported significantly higher IFN-γ levels in the cerebrospinal fluid from EV71 patients with pulmonary edema than in the cerebrospinal fluid from patients without pulmonary edema.[43] Our data also demonstrated that the frequency of IFN-γ-producing T cells varies, depending on time point post-infection and tissues infected. These differences highlight the dynamic balance that exists between the protective effects and the immune-pathogenic effects of IFN-γ during EV71 infection. This balance is dependent on the infection time course and the involved tissues and may help explain the seemingly conflicting results that have been reported regarding the role of IFN-γ during EV71 infection. Serum EV71-neutralizing antibody titers increased from PID 7 to PID 14 and peaked at PID 21 in the orally infected pigs. The same trend was observed in the combined oral–nasally infected pigs from PID 7 to PID 14, although the titer was much lower than in the orally infected pigs. Notably, one oral dose of the EV71 BJ110 strain without any adjuvant induced serum neutralizing antibody titers significantly higher than those observed in human patients.[44] Importantly, these titers were comparable to those achieved by multiple high doses of current candidate vaccines that

contain no adjuvants and are administered via non-oral immunization.[45,46] Therefore, oral challenge of neonatal gnotobiotic pigs with the EV71 BJ110 strain is highly immunogenic. This finding suggests that attenuated EV71 has potential as an oral EV71 vaccine candidate. This high immunogenicity also renders the current gnotobiotic pig model suitable for EV71 vaccine evaluation.

By virtue of this report, the neonatal gnotobiotic pig model is one of the most comprehensively described animal models for EV71. The results presented here demonstrated that neonatal gnotobiotic pigs represent a suitable alternative animal model for the currently used mouse and non-human primate models for EV71. First, the observation of pulmonary hemorrhage and edema (although the causality of these symptoms is debatable), as well as neurological and respiratory signs in the orally infected neonatal gnotobiotic pigs, makes this pig model a unique neonatal animal model. A recent study in 3- to 3.5-year-old Rhesus macaques demonstrated that only mild lesions were present in the central nervous system and lungs after oral and respiratory route inoculation.[41] The results presented here indicate that pigs can model EV71 infection in humans as well as non-human primates. Second, the use of the neurovirulent EV71 BJ110 strain, which is a member of the C4 genotype, is important for the development of vaccines and therapeutics for the ongoing EV71 epidemic.[47] Third, no previous animal models for EV71 have been established using gnotobiotic animals. Our gnotobiotic pig model of EV71 infections allows for more specific studies of viral pathogenesis, immunogenicity and vaccine efficacy and for the development of antiviral therapies. Fourth, unlike studies in mice,[11,48] the EV71 strain used in this study has not undergone host adaption in pigs; thus, our gnotobiotic pig model more accurately reflects the pathogenicity of EV71 in humans. Taken together, pigs are a particularly attractive alternative animal species for an improved animal model of EV71 infection.

In summary, our study provides *in vitro* and *in vivo* evidence that neonatal gnotobiotic pigs can be orally and oral–nasally infected by the recently isolated, non-pig-adapted neurovirulent human EV71 BJ110 strain. Long-term shedding of high virus titers in fecal samples (i.e., up to 18 days post-infection, with a peak titer of 2.22×10^8 RNA copies/mL) and spreading of the virus from intestinal tissues to the central nervous system and to respiratory system tissues were observed. Infection resulted in the development of some HFMD clinical signs, as well as neurological and respiratory signs that mimic some symptoms of the severe EV71 diseases that occur in human infants. Significant changes in the frequencies of both $CD3^+CD4^+IFN\text{-}\gamma^+$ and $CD3^+CD8^+IFN\text{-}\gamma^+$ T cells were detected in the lungs and brain tissues on PID 7 and PID 14. High serum EV71-neutralizing antibody titers were also induced in both orally and combined oral–nasally infected pigs. Together, these results demonstrate that neonatal gnotobiotic pigs represent a promising novel animal model species for the preclinical evaluation of vaccines and antiviral drugs, as well as for elucidating the underlying mechanisms of pathogenesis during EV71 infection in humans.

ACKNOWLEDGMENTS

We thank Pete Jobst, Andrea Pulliam, Kim Allen and Shannon Viers (Virginia-Maryland College of Veterinary Medicine, Virginia Tech) for their excellent animal care. We thank Melissa Makris (Virginia-Maryland College of Veterinary Medicine, Virginia Tech) for assistance with flow cytometry. The study was partially supported by Fralin Funds of the Fralin Life Science Institute at Virginia Tech.

1 Ooi MH, Wong SC, Lewthwaite P, Cardosa MJ, Solomon T. Clinical features, diagnosis, and management of enterovirus 71. *Lancet Neurol* 2010; **9**: 1097–1105.
2 Zeng M, El Khatib NF, Tu S *et al*. Seroepidemiology of Enterovirus 71 infection prior to the 2011 season in children in Shanghai. *J Clin Virol* 2012; **53**: 285–289.
3 Ho M, Chen ER, Hsu KH *et al*. An epidemic of enterovirus 71 infection in Taiwan. Taiwan Enterovirus Epidemic Working Group. *N Engl J Med* 1999; **341**: 929–935.
4 Xing W, Liao Q, Viboud C *et al*. Hand, foot, and mouth disease in China, 2008–12: an epidemiological study. *Lancet Infect Dis* 2014; **14**: 308–318.
5 Hashimoto I, Hagiwara A. Studies on the pathogenesis of and propagation of enterovirus 71 in Poliomyelitis-like disease in monkeys. *Acta Neuropathol* 1982; **58**: 125–132.
6 Hashimoto I, Hagiwara A, Kodama H. Neurovirulence in cynomolgus monkeys of enterovirus 71 isolated from a patient with hand, foot and mouth disease. *Arch Virol* 1978; **56**: 257–261.
7 Arita M, Shimizu H, Nagata N *et al*. Temperature-sensitive mutants of enterovirus 71 show attenuation in cynomolgus monkeys. *J Gen Virol* 2005; **86**: 1391–1401.
8 Dong C, Liu L, Zhao H *et al*. Immunoprotection elicited by an enterovirus type 71 experimental inactivated vaccine in mice and rhesus monkeys. *Vaccine* 2011; **29**: 6269–6275.
9 Lin YL, Yu CI, Hu YC *et al*. Enterovirus type 71 neutralizing antibodies in the serum of macaque monkeys immunized with EV71 virus-like particles. *Vaccine* 2012; **30**: 1305–1312.
10 Nie K, Zhang Y, Luo L *et al*. Visual detection of human enterovirus 71 subgenotype C4 and Coxsackievirus A16 by reverse transcription loop-mediated isothermal amplification with the hydroxynaphthol blue dye. *J Virol Methods* 2011; **175**: 283–286.
11 Wang YF, Chou CT, Lei HY *et al*. A mouse-adapted enterovirus 71 strain causes neurological disease in mice after oral infection. *J Virol* 2004; **78**: 7916–7924.
12 Khong WX, Yan B, Yeo H *et al*. A non-mouse-adapted enterovirus 71 (EV71) strain exhibits neurotropism, causing neurological manifestations in a novel mouse model of EV71 infection. *J Virol* 2012; **86**: 2121–2131.
13 Liu J, Dong W, Quan X *et al*. Transgenic expression of human P-selectin glycoprotein ligand-1 is not sufficient for enterovirus 71 infection in mice. *Arch Virol* 2012; **157**: 539–543.
14 Meurens F, Summerfield A, Nauwynck H, Saif L, Gerdts V. The pig: a model for human infectious diseases. *Trends Microbiol* 2012; **20**: 50–57.
15 Ward LA, Rosen BI, Yuan L, Saif LJ. Pathogenesis of an attenuated and a virulent strain of group A human rotavirus in neonatal gnotobiotic pigs. *J Gen Virol* 1996; **77**: 1431–1441.
16 Yuan L, Wen K, Azevedo MS *et al*. Virus-specific intestinal IFN-gamma producing T cell responses induced by human rotavirus infection and vaccines are correlated with protection against rotavirus diarrhea in gnotobiotic pigs. *Vaccine* 2008; **26**: 3322–3331.
17 Yuan L, Saif LJ. Induction of mucosal immune responses and protection against enteric viruses: rotavirus infection of gnotobiotic pigs as a model. *Vet Immunol Immunopathol* 2002; **87**: 147–160.
18 Wen K, Li G, Bui T *et al*. High dose and low dose *Lactobacillus acidophilus* exerted differential immune modulating effects on T cell immune responses induced by an oral human rotavirus vaccine in gnotobiotic pigs. *Vaccine* 2012; **30**: 1198–1207.
19 Souza M, Costantini V, Azevedo MS, Saif LJ. A human norovirus-like particle vaccine adjuvanted with ISCOM or mLT induces cytokine and antibody responses and protection to the homologous GII.4 human norovirus in a gnotobiotic pig disease model. *Vaccine* 2007; **25**: 8448–8459.
20 Nishimura Y, Shimojima M, Tano Y *et al*. Human P-selectin glycoprotein ligand-1 is a functional receptor for enterovirus 71. *Nat Med* 2009; **15**: 794–797.
21 Yamayoshi S, Yamashita Y, Li J *et al*. Scavenger receptor B2 is a cellular receptor for enterovirus 71. *Nat Med* 2009; **15**: 798–801.
22 Yang B, Chuang H, Yang KD. Sialylated glycans as receptor and inhibitor of enterovirus 71 infection to DLD-1 intestinal cells. *Virol J* 2009; **6**: 141.
23 Baisse B, Galisson F, Giraud S, Schapira M, Spertini O. Evolutionary conservation of P-selectin glycoprotein ligand-1 primary structure and function. *BMC Evol Biol* 2007; **7**: 166.
24 Kim JW, Zhao SH, Uthe JJ, Bearson SM, Tuggle CK. Assignment of the scavenger receptor class B, member 2 gene (*SCARB2*) to porcine chromosome 8q11-->q12 by somatic cell and radiation hybrid panel mapping. *Cytogenet Genome Res* 2006; **112**: 342H.
25 Liu F, Li G, Wen K *et al*. Porcine small intestinal epithelial cell line (IPEC-J2) of rotavirus infection as a new model for the study of innate immune responses to rotaviruses and probiotics. *Viral Immunol* 2010; **23**: 135–149.
26 Yuan L, Ward LA, Rosen BI, To TL, Saif LJ. Systematic and intestinal antibody-secreting cell responses and correlates of protective immunity to human rotavirus in a gnotobiotic pig model of disease. *J Virol* 1996; **70**: 3075–3083.
27 Tan EL, Yong LL, Quak SH *et al*. Rapid detection of enterovirus 71 by real-time TaqMan RT-PCR. *J Clin Virol* 2008; **42**: 203–206.
28 Meyer RC, Bohl EH, Kohler EM. Procurement and maintenance of germ-free seine for microbiological investigations. *Appl Microbiol* 1964; **12**: 295–300.
29 Yuan L, Ishida S, Honma S *et al*. Homotypic and heterotypic serum isotype-specific antibody responses to rotavirus nonstructural protein 4 and viral protein (VP) 4, VP6, and VP7 in infants who received selected live oral rotavirus vaccines. *J Infect Dis* 2004; **189**: 1833–1845.
30 Plevka P, Perera R, Cardosa J, Kuhn RJ, Rossmann MG. Crystal structure of human enterovirus 71. *Science* 2012; **336**: 1274.
31 Wang X, Peng W, Ren J *et al*. A sensor-adaptor mechanism for enterovirus uncoating from structures of EV71. *Nat Struct Mol Biol* 2012; **19**: 424–429.
32 Solomon T, Lewthwaite P, Perera D *et al*. Virology, epidemiology, pathogenesis, and control of enterovirus 71. *Lancet Infect Dis* 2010; **10**: 778–790.

33 Weng KF, Chen LL, Huang PN, Shih SR. Neural pathogenesis of enterovirus 71 infection. *Microbes Infect* 2010; **12**: 505–510.
34 Wang SM, Lei HY, Huang KJ *et al*. Pathogenesis of enterovirus 71 brainstem encephalitis in pediatric patients: roles of cytokines and cellular immune activation in patients with pulmonary edema. *J Infect Dis* 2003; **188**: 564–570.
35 Wong KT, Munisamy B, Ong KC *et al*. The distribution of inflammation and virus in human enterovirus 71 encephalomyelitis suggests possible viral spread by neural pathways. *J Neuropathol Exp Neurol* 2008; **67**: 162–169.
36 Wen YY, Chang TY, Chen ST, Li C, Liu HS. Comparative study of enterovirus 71 infection of human cell lines. *J Med Virol* 2003; **70**: 109–118.
37 Lin TY, Hsia SH, Huang YC, Wu CT, Chang LY. Proinflammatory cytokine reactions in enterovirus 71 infections of the central nervous system. *Clin Infect Dis* 2003; **36**: 269–274.
38 Chang LY, Tsao KC, Hsia SH *et al*. Transmission and clinical features of enterovirus 71 infections in household contacts in Taiwan. *JAMA* 2004; **291**: 222–227.
39 Cerf-Bensussan N, Gaboriau-Routhiau V. The immune system and the gut microbiota: friends or foes? *Nat Rev Immunol* 2010; **10**: 735–744.
40 Hsueh C, Jung SM, Shih SR *et al*. Acute encephalomyelitis during an outbreak of enterovirus type 71 infection in Taiwan: report of an autopsy case with pathologic, immunofluorescence, and molecular studies. *Mod Pathol* 2000; **13**: 1200–1205.
41 Zhang Y, Cui W, Liu L *et al*. Pathogenesis study of enterovirus 71 infection in rhesus monkeys. *Lab Invest* 2011; **91**: 1337–1350.
42 Chang LY, Hsiung CA, Lu CY *et al*. Status of cellular rather than humoral immunity is correlated with clinical outcome of enterovirus 71. *Pediatr Res* 2006; **60**: 466–471.
43 Wang SM, Lei HY, Su LY *et al*. Cerebrospinal fluid cytokines in enterovirus 71 brain stem encephalitis and echovirus meningitis infections of varying severity. *Clin Microbiol Infect* 2007; **13**: 677–682.
44 Yang C, Deng C, Wan J, Zhu L, Leng Q. Neutralizing antibody response in the patients with hand, foot and mouth disease to enterovirus 71 and its clinical implications. *Virol J* 2011; **8**: 306.
45 Zhu FC, Wang JZ, Li XL *et al*. Reactogenicity and immunogenicity of an enterovirus 71 vaccine in Chinese healthy children and infants. *Pediatr Infect Dis J* 2012; **31**: 1158–1165.
46 Li YP, Liang ZL, Gao Q *et al*. Safety and immunogenicity of a novel human Enterovirus 71 (EV71) vaccine: a randomized, placebo-controlled, double-blind, Phase I clinical trial. *Vaccine* 2012; **30**: 3295–3303.
47 Yan XF, Gao S, Xia JF *et al*. Epidemic characteristics of hand, foot, and mouth disease in Shanghai from 2009 to 2010: Enterovirus 71 subgenotype C4 as the primary causative agent and a high incidence of mixed infections with coxsackievirus A16. *Scand J Infect Dis* 2012; **44**: 297–305.
48 Wang W, Duo J, Liu J *et al*. A mouse muscle-adapted enterovirus 71 strain with increased virulence in mice. *Microbes Infect* 2011; **13**: 862–870.

Supplementary Information for this article can be found on *Emerging Microbes & Infections*' website (http://www.nature.com/emi/)